

# Spatialized Bayesian inference and uncertainty quantification on constrained co-domains with Gaussian Processes.

Application to the simplex.

**Lucas Drumetz**

lucas.drumetz@imt-atlantique.fr

IMT Atlantique, Dept. Mathematical and Electrical Engineering, Lab-STICC,  
Brest, France

MASCOT-NUM, ENSAI, Rennes, 1-3 April 2026



GENerative modeling with kErnelS for Inverse problemS

CLUSTER  
SEQUOIA



UQ in Bayesian inverse problems in imaging:

- ▶ Sample spatialized posterior distributions with generative models as priors
- ▶ Learn prior distributions from data
- ▶ Handle constrained valued-images

Example applications:

- ▶ Interpolation/forecasting of oceanic variables at the global scale
- ▶ Source separation in optical remote sensing
- ▶ Geometric ML

→ This presentation: handling UQ for images with constrained values, using Gaussian Processes.

*Aitchison Geometry on the Simplex for Uncertainty Quantification in Bayesian Hyperspectral Image Unmixing*, H. Blondel, L. Drumetz, T. Chonavel., Submitted to IEEE ICIP 2026.

# Outline

## Bayesian modeling on constrained valued images

- Problem Statement

- Application to the simplex: spectral unmixing

## Gaussian Processes on constrained domains

- Aitchison geometry on the simplex

- Pushforward Gaussian distribution

- Spatialized Bayesian Unmixing

- Inference and UQ

# Bayesian inverse problems

Recover parameter  $\mathbf{x} \in \mathbb{R}^N$  given observations  $\mathbf{y} \in \mathbb{R}^n$  (typically  $n < N$ ), a forward model and a prior distribution on  $\mathbf{x}$ .

$$p_{X|Y}(\mathbf{x}|\mathbf{y}) \propto p_{Y|X}(\mathbf{y}|\mathbf{x})p_X(\mathbf{x})$$

Classically,  $p_{X|Y}(\mathbf{x}|\mathbf{y})$  has a closed form but it is intractable, but requires:

- ▶ Sampling algorithms
- ▶ Variational inference

to compute expectations using  $M$  i.i.d. samples from the posterior:

$$\mathbb{E}[f(X)|Y = y] = \int_{\mathbb{R}^n} f(\mathbf{x})p_{X|Y}(\mathbf{x}|\mathbf{y})d\mathbf{x} \approx \frac{1}{M} \sum_{i=1}^M f(\mathbf{x}_i)$$

→ obtain posterior averages, covariances... For example, taking  $f = \text{Id}$ , we get the posterior mean:

$$\mathbb{E}[X|Y = y] = \int_{\mathbb{R}^n} \mathbf{x}p_{X|Y}(\mathbf{x}|\mathbf{y})d\mathbf{x} \approx \frac{1}{M} \sum_{i=1}^M \mathbf{x}_i$$

which is the minimum (Euclidean) mean square error estimator.

# Objectives/requirements

In this talk,  $\mathbf{x}$  and  $\mathbf{y}$  are spatialized and are observed at locations  $\mathbf{u} \in \mathbb{R}^d$ .

$$\mathbf{x} \in \mathcal{C}^N, \quad \mathbf{y} \in \mathcal{D}^n,$$

for some  $\mathcal{C} \subset \mathbb{R}^P, \mathcal{D} \subseteq \mathbb{R}^L$

- ▶ We want to be able to include any location  $\mathbf{u} \in \mathbb{R}^q$  inside  $\mathbf{x}$  (In imaging, typically locations are on a grid)
- ▶  $\mathbf{y}$  can be observations of the same quantity at some locations, or live in another space entirely.
- ▶ We want to handle constrained  $\mathbf{x}$ , i.e. images with constrained values.
- ▶ Need for a parametric prior distribution of  $\mathbf{x}$  to handle spatial correlations

# Constrained inference

Assumption:  $\mathcal{C} \subset \mathbb{R}^P$  is diffeomorphic to a Euclidean space  $\mathbb{R}^D$ , i.e. there exists a diffeomorphism  $\phi : \mathcal{C} \rightarrow \mathbb{R}^D$ .

$$\mathbf{z} = \phi(\mathbf{x})$$

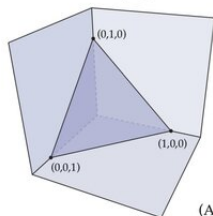
This encompasses many sets of practical interest:

- ▶ The *strictly* positive orthant  $\{\mathbf{x} \in \mathbb{R}^P, x_i > 0\}$
- ▶ **The interior of the probability simplex with  $P$  vertices**,  
 $\Delta_{P-1} = \{\mathbf{x} \in \mathbb{R}^P, x_i > 0, \sum_{i=1}^P x_i = 1\}$  and variants
- ▶ The *interior* of the unit disk:  $\{\mathbf{x} \in \mathbb{R}^P, \|\mathbf{x}\| < 1\}$
- ▶ The set of symmetric positive definite matrices:  
 $\{\mathbf{X} \in \mathbb{R}^{P \times P}, \forall \mathbf{v} \in \mathbb{R}^P, \mathbf{v}^T \mathbf{X} \mathbf{v} > 0\}$
- ▶ and others...

# Running Example: the probability simplex

**Definition.** The *standard  $n$ -simplex* is the collection of points

$$\sigma := \left\{ (x_0, \dots, x_n) \in \mathbb{R}^{n+1} \mid \sum_{i=0}^n x_i = 1, x_i \geq 0 \forall i \right\}.$$



(Also known as the “probability simplex.”)

2-simplex and its natural embedding in  $\mathbb{R}^3$ . From [Zheng et al, AAI, 2026]

Applications:

- ▶ compositional data analysis
- ▶ modeling categorical probability distributions (e.g. classification)
- ▶ spectral unmixing

# Related work

- ▶ Manifold-valued GP for SPD matrices/punctured sphere <sup>1</sup>
- ▶ Generative models on the simplex (flow matching/GP) with the same idea <sup>2</sup>(very recent!)

Our work:

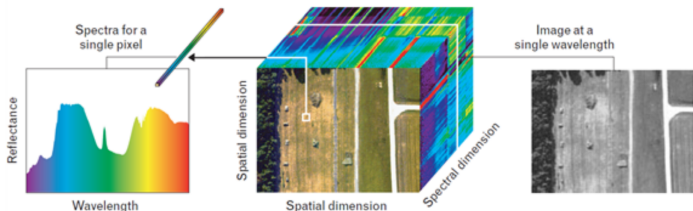
- ▶ Generic construction of GP with values in constrained sets
- ▶ Application to the simplex and source separation
- ▶ Geometric implications
- ▶ Geometry-compliant UQ metrics and visualization for  $P = 3$ .

---

<sup>1</sup>A. Mallasto and A. Feragen. Wrapped gaussian process regression on riemannian manifolds. In Proceedings of the IEEE Conference on Computer Vision and Pattern Recognition, pages 5580–5588, 2018.

<sup>2</sup>Williams, B., Tetali, H. V., Klami, A., & Hartmann, M. (2026). Simplex-to-Euclidean Bijection for Conjugate and Calibrated Multiclass Gaussian Process. arXiv preprint arXiv:2603.16621.

# Hyperspectral imaging



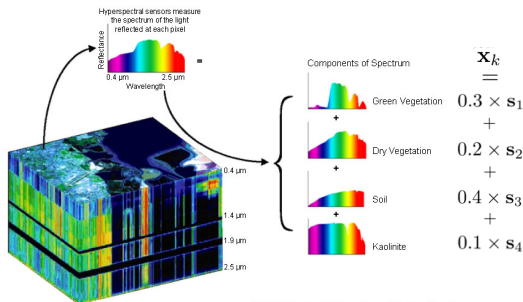
Hyperspectral imaging concept.

- ▶ Each pixel: reflectance spectrum for many contiguous and narrow wavelengths (visible and near-IR).
- ▶ Also a collection of gray-level reflectance images for each wavelength.
- ▶ The spectrum characterizes a material, but because of the limited spatial resolution, mixed pixels are present.

Applications in: **Remote sensing** – environment monitoring, geology, precision agriculture, planetary science, defense ...

but also food processing, chemometrics, document analysis...

# Spectral Unmixing



(NEMO Project Office, United States Navy)

## Linear Spectral Unmixing

A blind source separation problem<sup>3</sup> whose goals are to:

- ▶ extract the signatures of the *materials (endmembers)* in the image
- ▶ estimate their *relative proportions (fractional abundances)* in each pixel.

<sup>3</sup>Bioucas-Dias, J. M., Plaza, A., Dobigeon, N., Parente, M., Du, Q., Gader, P., & Chanussot, J. (2012). Hyperspectral unmixing overview: Geometrical, statistical, and sparse regression-based approaches. IEEE journal of selected topics in applied earth observations and remote sensing, 5(2), 354-379.

# Spectral Unmixing

Each pixel  $\mathbf{y}_n \in \mathbb{R}^L$  of the image is decomposed as:

$$\mathbf{y}_n = \mathbf{S}\mathbf{x}_n + \mathbf{e}_n$$

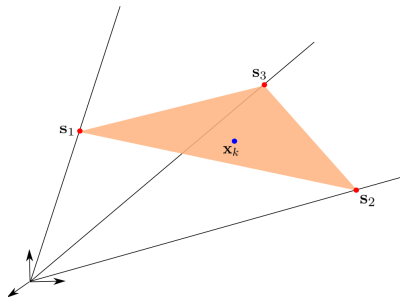
with  $\mathbf{x}_n \in \Delta_{P-1}$  for all  $n$ . [Bioucas-Dias et al. 2012]

$$\mathbf{Y} = \mathbf{S}\mathbf{X} + \mathbf{E}$$

with  $\mathbf{Y} = [\mathbf{y}_1, \mathbf{y}_2, \dots, \mathbf{y}_N] \in \mathbb{R}^{L \times N}$ ,  $\mathbf{E} \in \mathbb{R}^{L \times N}$  i.i.d Gaussian noise,  $\mathbf{S} \in \mathbb{R}^{L \times P}$  and  $\mathbf{X} \in \Delta_{P-1}^N \subset \mathbb{R}^{P \times N}$ .

$L$ : number of wavelengths  
 $N$ : number of pixels  
 $P$ : number of endmembers

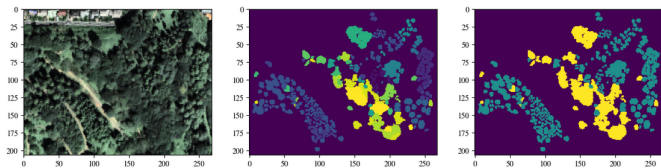
$\mathbf{Y}$ : data matrix  
 $\mathbf{S}$ : endmember matrix  
 $\mathbf{X}$ : abundance matrix



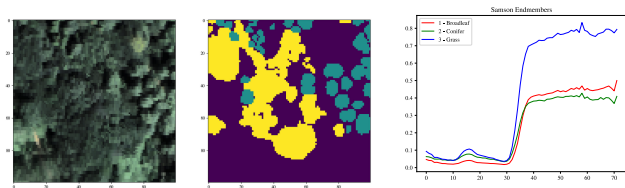
Geometric interpretation of the noiseless Linear SU problem, in the case of 3 endmembers in a 3D ambient space.

# Data and problem

Tama Forest Garden, near Tokyo, Japan. 72 spectral bands (wavelengths) in the visible and near infrared. 1m spatial resolution. Partial (classification) GT.<sup>4</sup>



RGB image (left), GT for several tree species (middle), organized into broadleaf (yellow) and conifer trees (green)



100×100 crop. We see that the sensor introduces spatial artifacts.

Task: separate conifer, broadleaf trees, grass (1 signature given per material).

<sup>4</sup>T. Matsuki, N. Yokoya, and A. Iwasaki, "Hyperspectral tree species classification of japanese complex mixed forest with the aid of lidar data," IEEE JSTARS, vol. 8, no. 5, pp. 2177–2187, May 2015.

# Spectral Unmixing processing chain

- ▶ Blind setup:  $P, \mathbf{S}, \mathbf{X}$  unknown  $\rightarrow$  elegant but unrealistic
- ▶ "Supervised setup": Here,  $\mathbf{S}$  is known or partially known

Need for ecology, environmental monitoring, planetology... But very ill posed problem:

- ▶ Variability of  $\mathbf{S}$
- ▶ Proximity/correlation between materials in practical scenarios.
- ▶ Ground truth is scarce, expensive and unreliable for remote sensing images.

Classically: Constrained Least Square estimation (MAP) of  $\mathbf{x}_n$ , in each pixel:

$$\hat{\mathbf{X}} = \mathbf{x}_{\in \Delta_{P-1}} \operatorname{Narg} \min \|\mathbf{Y} - \mathbf{S}\mathbf{X}\|_F^2$$

Need for tools and diagnostics for feasibility, assessing the difficulty of the problem for practitioners.

# Bayesian modeling for spectral unmixing

$$p_{X|Y}(\mathbf{x}|\mathbf{y}) \propto p_{Y|X}(\mathbf{y}|\mathbf{x})p_X(\mathbf{x})$$

with  $p_{Y|X}(\mathbf{y}|\mathbf{x}) \sim \mathcal{N}(\mathbf{y}; \mathbf{S}\mathbf{x}, \sigma^2\mathbf{I}_L)$  and  $p_X(\mathbf{x}) \sim \text{Dir}(\boldsymbol{\alpha})$

But the posterior samples on  $\mathbf{x}$  are

- ▶ Typically underexploited: No UQ diagnostics, just MMSE Estimators<sup>5</sup>.
- ▶ Results in cropped posterior distributions on the simplex: e.g. Truncated Gaussian for  $\boldsymbol{\alpha} = \mathbf{1}$  (Uniform prior)
- ▶ Dirichlet allows mass on the boundary and is tied to the Euclidean Geometry of the simplex.
- ▶ all variables are usually assumed i.i.d. spatially: not robust to noise.

---

<sup>5</sup>Eches, O., Dobigeon, N., Mailhes, C., & Tournet, J. Y. (2010). Bayesian estimation of linear mixtures using the normal compositional model. Application to hyperspectral imagery. IEEE Transactions on Image Processing, 19(6), 1403-1413.

# Outline

## Bayesian modeling on constrained valued images

- Problem Statement

- Application to the simplex: spectral unmixing

## Gaussian Processes on constrained domains

- Aitchison geometry on the simplex

- Pushforward Gaussian distribution

- Spatialized Bayesian Unmixing

- Inference and UQ

# Compositional Data Analysis: Aitchison geometry

Well known in geostatistics<sup>6</sup> but not at all in the signal processing community.

Define the centered log-ratio transform  $\text{clr} : \text{int } \Delta_{P-1} \rightarrow \mathbb{R}^{P-1}$  as

$$\mathbf{w} = \psi(\mathbf{x}) \triangleq \text{clr}(\mathbf{x}) := \left[ \log x_p - \frac{1}{P} \sum_{k=1}^P \log x_k \right]_{p=1, \dots, P}$$

The image of the simplex is the hyperplane  $\mathbf{1}^T \mathbf{u} = 0$ .

Choosing an orthonormal basis  $\mathbf{H} \in \mathbb{R}^{P \times P-1}$ , we get a true bijection, called "isometric log ratio",  $\text{ilr}$ :

$$\mathbf{z} = \phi(\mathbf{x}) = \text{ilr}(\mathbf{x}) \triangleq \mathbf{H}^T \mathbf{w}$$

And the inverse is given by

$$\text{ilr}^{-1}(\mathbf{z}) = \text{softmax}(\mathbf{H}\mathbf{z}) = \left[ \frac{\exp w_p}{\sum_{k=1}^P \exp(w_k)} \right]_{p=1, \dots, P}.$$

---

<sup>6</sup>Aitchison, J. (1982). The statistical analysis of compositional data. Journal of the Royal Statistical Society: Series B (Methodological), 44(2), 139-160.

# Pushforward Gaussian prior

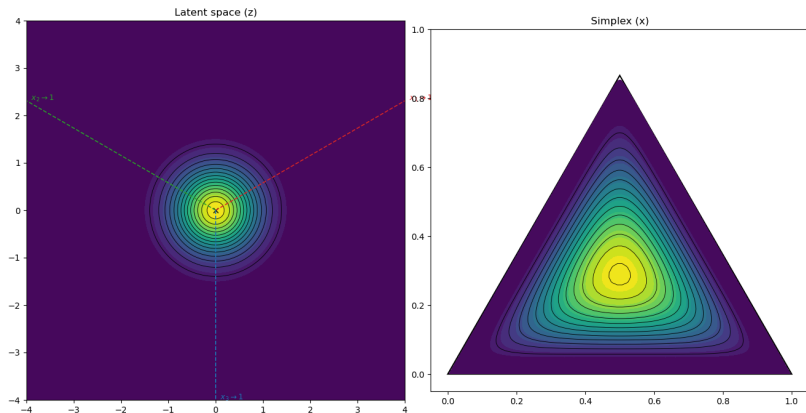
Now we have a diffeomorphism  $\phi : \mathcal{C} \rightarrow \mathbb{R}^d$ , we can put a Gaussian prior on  $\mathbf{z}$  and push it to  $\mathcal{C}$  using  $\phi^{-1}$ .

$$\mathbf{z} \sim \mathcal{N}(\boldsymbol{\mu}, \boldsymbol{\Sigma})$$

Simplex example: defines a family of distributions in  $\Delta_{p-1}$  such that:

- ▶ Zero mass is put on the boundary  $\rightarrow$  same for the posterior
- ▶ Can be made permutation invariant (uninformative) if  $\boldsymbol{\Sigma} = \sigma^2 \mathbf{I}_{p-1}$
- ▶ May be multimodal depending on the latent prior.

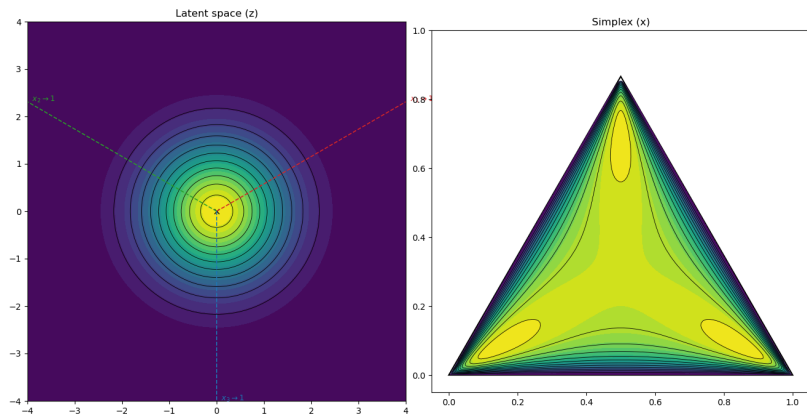
# Examples of ilr-Gaussian distributions ( $P = 3$ )



$$\mathbf{z} \sim \mathcal{N}(\mathbf{0}, \sigma^2 \mathbf{I}_{P-1})$$
$$\sigma^2 = 0.6$$

Zero mean and isotropic latent  $\rightarrow$  permutation invariant in the simplex

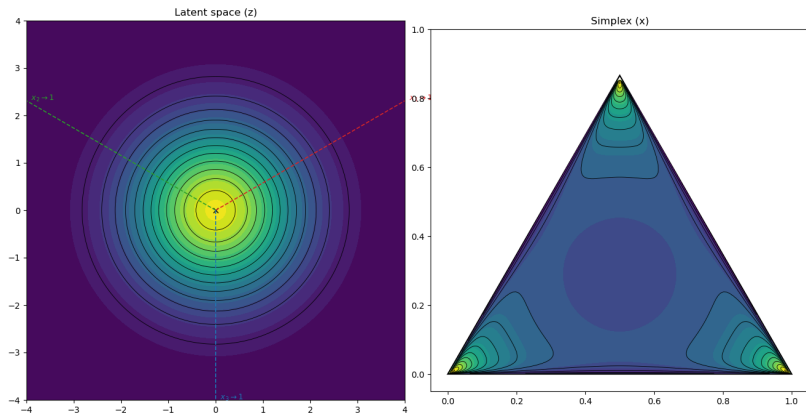
# Examples of $l_r$ -Gaussian distributions ( $P = 3$ )



$$\mathbf{z} \sim \mathcal{N}(\mathbf{0}, \sigma^2 \mathbf{I}_{P-1})$$
$$\sigma^2 = 1$$

Multimodal for large enough  $\sigma$  (still isotropic)

# Examples of ilr-Gaussian distributions ( $P = 3$ )

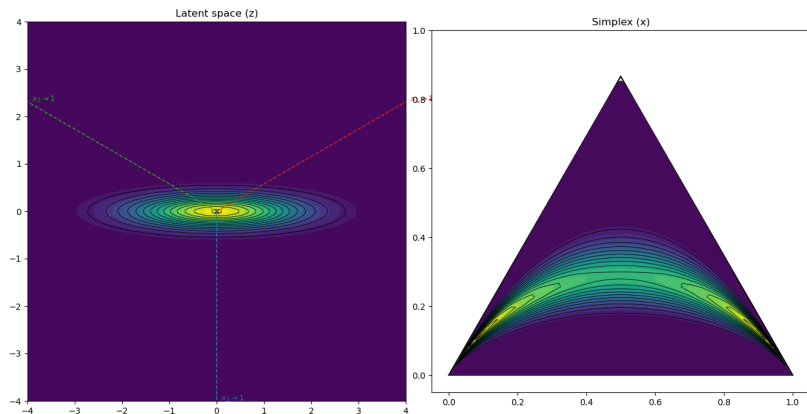


$$\mathbf{z} \sim \mathcal{N}(\mathbf{0}, \sigma^2 \mathbf{I}_{P-1})$$

$$\sigma^2 = 1.25$$

For large values of  $\sigma$ , distributions favor edges with equal probability.

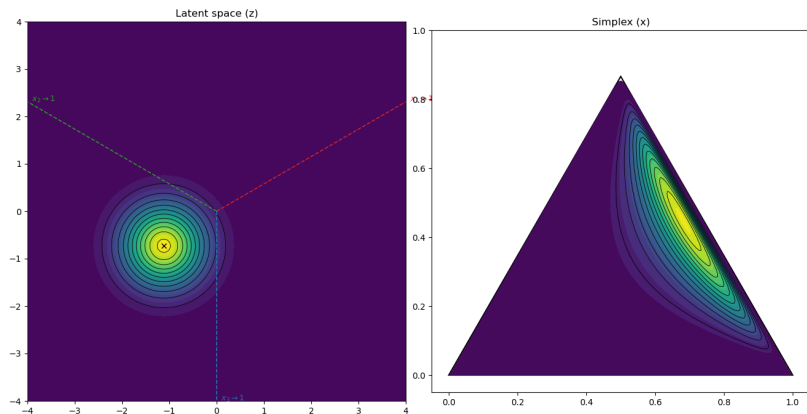
# Examples of ilr-Gaussian distributions ( $P = 3$ )



$$\mathbf{z} \sim \mathcal{N}\left(\mathbf{0}, \begin{bmatrix} \sigma_1^2 & 0 \\ 0 & \sigma_2^2 \end{bmatrix} \mathbf{I}_{P-1}\right)$$
$$\sigma_1^2 = 1, \sigma_2^2 = 0.2$$

For non isotropic covariances, behavior is more complex.

# Examples of $l_r$ -Gaussian distributions ( $P = 3$ )



$$\mathbf{z} \sim \mathcal{N}(\boldsymbol{\mu}, \sigma^2 \mathbf{I}_{P-1})$$
$$\sigma^2 = 0.6$$

The mean also affects how mass distributes in the simplex.

# Gaussian Process regression for constrained fields

Working in  $\mathbf{z}$ -space allows Gaussian priors on matrix  $\mathbf{Z} \in \mathbb{R}^{(P-1) \times N}$  ( $N$  latent values) at target locations  $\mathbf{u}_n \in \mathbb{R}^q$ ,  $n = 1, \dots, N$

Control spatial correlations via separable covariances in space and simplex dimensions:

$$\mathbf{X} = \psi(\mathbf{X}) \sim \mathcal{MN}(\mathbf{0}_{(P-1) \times N}, \sigma_a^2 \mathbf{I}_{P-1}, \mathbf{K}_U). \quad (1)$$

$\mathbf{K}_U$  encodes spatial correlations (i.e. a discretized Gaussian process):  $\mathbf{K}_{U_{i,j}} = k(\mathbf{u}_i, \mathbf{u}_j)$  for a given kernel function.

- ▶ Latent components are uncorrelated between one another:

$$\text{Cov}(\mathbf{x}_i, \mathbf{x}_j) = \mathbf{0}_N \quad \text{if } i \neq j$$

- ▶ For any given component, spatial correlation is governed by the kernel:

$$\text{Cov}(\mathbf{x}_i, \mathbf{x}_i) = \sigma_a^2 \mathbf{K}_U$$

Equivalently

$$\mathbf{x} = \text{vec}(\mathbf{X}) \sim (\mathbf{0}_{(P-1)N}, \sigma_a^2 \mathbf{I}_{(P-1)} \otimes \mathbf{K}_U)$$

# Latent GP prior for spatial interpolation on $\mathcal{C}$

Assuming observations  $\mathbf{y} = \text{vec}(\mathbf{Y}) \in \mathbb{R}^{PN}$  are also  $\mathcal{C}$ -valued, the likelihood can be written in latent space. If in addition we assume that the noise is additive and Gaussian there:

$$p_{\phi(Y)|Z}(\phi(\mathbf{y})|\mathbf{z}) = \mathcal{N}(\phi(\mathbf{y}); \boldsymbol{\mu}, \sigma^2 \mathbf{I}_{PN})$$

Then the prior is conjugate in  $\mathbf{z}$ -space and the posterior has a closed form in latent space:

$$p_{Z|\phi(Y)}(\mathbf{z}|\phi(\mathbf{y})) \propto p_{Y|Z}(\phi(\mathbf{y})|\mathbf{z})p_Z(\mathbf{z}) \sim \mathcal{N}(\mathbf{z}|\boldsymbol{\mu}_{Z|Y}, \boldsymbol{\Sigma}_{Z|Y})$$

is Gaussian and the moments are obtained in closed-form (GP regression in latent space).

This covers denoising or interpolation/extrapolation of signals with values on  $\mathcal{C}$ , assuming additive noise in latent space.

# Latent GP prior for Inverse problems

If the likelihood is specified in  $\mathbf{x}$ -space, the situation is more complex.

We can rewrite Bayes' theorem for the unconstrained variable  $\mathbf{z}$ :

$$p_{\mathbf{Z}|\mathbf{Y}}(\mathbf{z}|\mathbf{y}) \propto p_{\mathbf{Y}|\mathbf{Z}}(\mathbf{y}|\phi^{-1}(\mathbf{z}))p_{\mathbf{Z}}(\mathbf{z})$$

In our unmixing case on the simplex, for the whole matrix:

$$-\log p_{\mathbf{X}|\mathbf{Y}}(\mathbf{X}|\mathbf{Y}) = \frac{1}{2\sigma^2} \|\mathbf{Y} - \mathbf{S}\mathbf{X}\|_F^2 + \frac{1}{2\sigma_s^2} \|\phi(\mathbf{X})\mathbf{K}_U^{-1/2}\|_F^2 + \text{cst}$$

However, better to work in  $\mathbf{Z}$  space, since  $\mathbf{Z}$  is unconstrained:

$$-\log p_{\mathbf{Z}|\mathbf{Y}}(\mathbf{Z}|\mathbf{Y}) = \frac{1}{2\sigma^2} \|\mathbf{Y} - \mathbf{S}\phi^{-1}(\mathbf{Z})\|_F^2 + \frac{1}{2\sigma_s^2} \|\mathbf{Z}\mathbf{K}_U^{-1/2}\|_F^2 + \text{cst}$$

Here the likelihood and the prior live in different spaces: no closed form inference. Sampling is needed.

# Inference

We need constrained sampling algorithms to obtain samples of  $\mathbf{x}$  and compute the posterior mean (MMSE estimator):

$$\mathbb{E}[X|Y = y] = \int_{\mathbb{R}^n} \mathbf{x} p_{X|Y}(\mathbf{x}|y) d\mathbf{x} \approx \frac{1}{M} \sum_{i=1}^M \mathbf{x}_i$$

Inference can also be done in  $\mathbf{z}$ -space, using the same samples:

$$\mathbb{E}[Z|Y = y] = \int_{\mathbb{R}^d} \mathbf{z} p_{Z|Y}(\mathbf{z}|y) d\mathbf{z} \approx \frac{1}{M} \sum_{i=1}^M \mathbf{z}_i$$

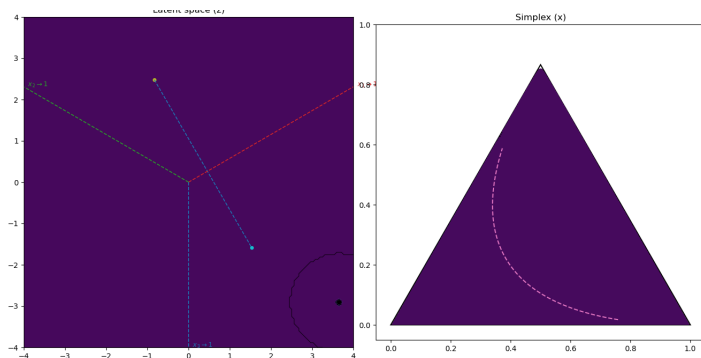
$\phi$  makes  $\mathcal{C}$  a (globally flat) Riemannian manifold structure with a pullback metric  $g = \phi^* \delta$ , where  $\delta$  is the Euclidean metric on  $\mathbb{R}^d$ . In particular this defines a geodesic distance:

$$d_\phi(\mathbf{x}_1, \mathbf{x}_2) = \|\phi(\mathbf{x}_1) - \phi(\mathbf{x}_2)\|_2^2 = \|\mathbf{z}_1 - \mathbf{z}_2\|_2^2$$

for which  $\phi^{-1}(\mathbb{E}[Z|Y = y])$  is the geodesic MMSE estimator of  $\mathbf{x}$ .

Not clear which is better (if  $\mathcal{C}$  is convex, at least both remain in  $\mathcal{C}$ ).

# In the simplex: Aitchison distance vs Euclidean distance



Aitchison geodesic in the simplex. The geodesic is a straight line in latent space.

- ▶ Geodesics are straight lines in latent space
- ▶ The ilr-Gaussian distribution has Gaussian Riemannian density  $d\nu_{\mathcal{C}}(\mathbf{x}) = \mathcal{N}(\phi(\mathbf{x}); \boldsymbol{\mu}, \boldsymbol{\Sigma})d\text{vol}_g(\mathbf{x})$ , but the corresponding density in the Euclidean geometry is corrected by the Jacobian of  $\phi$ :

$$d\nu_{\mathcal{C}}(\mathbf{x}) = \mathcal{N}(\phi(\mathbf{x}); \boldsymbol{\mu}, \boldsymbol{\Sigma})|\det(D\phi(\mathbf{x}))|d\mathbf{x}$$

# Constrained sampling

Also related to geometry.

Unconstrained  $\mathbf{x}$ : One can use the Unadjusted Langevin Algorithm:

$$\mathbf{x}_{t+1} = \mathbf{x}_t - \beta \nabla U(\mathbf{x}_t) + \sqrt{2\beta} \xi_t$$

where  $\xi_t \sim \mathcal{N}(\mathbf{0}, \mathbf{I})$ , and  $U(\mathbf{x}) = -\log(p_{X|Y}(\mathbf{x}|\mathbf{y}))$

For  $\mathbf{x}$  in  $\mathcal{C}$ , the posterior lives inside  $\Delta_{P-1}$ . Several options for sampling:

- ▶ Mirror Langevin<sup>7</sup> (simplex native): simple exponential updates on  $U(\mathbf{x})$
- ▶ Riemannian Langevin (directly uses the pullback geometry<sup>8</sup>):

$$\mathbf{z}_{t+1} = \mathbf{z}_t - \beta \nabla V(\mathbf{z}_t) + \sqrt{2\beta} \xi_t$$

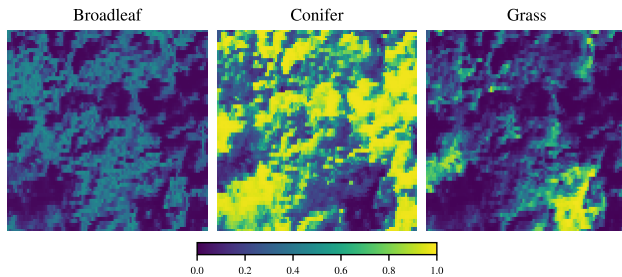
with  $V(\mathbf{z}) = -\log(p_{Z|Y}(\mathbf{z}|\mathbf{y}))$

---

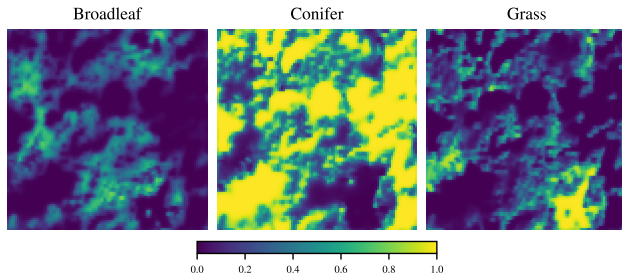
<sup>7</sup>Hsieh, Y. P., Kavis, A., Rolland, P., & Cevher, V. (2018). Mirrored langevin dynamics. Advances in Neural Information Processing Systems, 31.

<sup>8</sup>Wang, X., Lei, Q., & Panageas, I. (2020). Fast convergence of langevin dynamics on manifold: Geodesics meet log-sobolev. Advances in Neural Information Processing Systems, 33, 18894-18904.

# First order information



Geodesic mean for each component, dirac kernel



Geodesic mean for each component, with an exponential kernel

## Second order information: constrained UQ

UQ in constrained domains: covariance of posterior samples (for 1 pixel first)?

Same thing: covariances make sense both in  $\mathbf{x}$  and  $\mathbf{z}$  space:

$$\Sigma_X = \mathbb{E}[(X - \mu_X)(X - \mu_X)^T | Y], \quad \mu_X = \mathbb{E}[X | Y]$$

But:

- ▶ If  $\mathcal{C}$  is not fully dimensional in  $\mathbb{R}^d$ ,  $\Sigma_X$  will be singular.
- ▶ Gaussian approximations put mass outside  $\mathcal{C}$  and credible regions can be meaningless.

Defining covariance in  $\mathbf{Z}$ -space fixes both issues:

$$\Sigma_Z = \mathbb{E}[(Z - \mu_Z)(Z - \mu_Z)^T | Y], \quad \mu_Z = \mathbb{E}[Z | Y]$$

so that Gaussian approximations in  $\mathbf{z}$ -space make perfect sense.

# Credible regions in the simplex

For (unconstrained) Gaussian distributions in  $\mathbb{R}^d \mathcal{N}(\mathbf{x}|\boldsymbol{\mu}, \boldsymbol{\Sigma})$ , credible ellipsoid  $E_\alpha$  containing a proportion  $\alpha \in [0, 1]$  of the total mass:

$$E_\alpha = \{\mathbf{x} \in \mathbb{R}^n, (\mathbf{x} - \boldsymbol{\mu})\boldsymbol{\Sigma}^{-1}(\mathbf{x} - \boldsymbol{\mu}) < F_{\chi_d^2}^{-1}(\alpha)\}$$

- ▶ Gaussian approximation of  $p_{X|Y}(\mathbf{x}|\mathbf{y})$  in  $\mathbf{x}$ -space as a measure of uncertainty in the simplex can be misleading.
- ▶ Better strategy: Gaussian approximation of  $p_{Z|Y}(\mathbf{z}|\mathbf{y})$  in  $\mathbf{z}$ -space, and pushforward  $\alpha$ -credible ellipsoids to  $\mathcal{C}$  using  $\phi^{-1}$ : defines credible regions in  $\mathcal{C}$  with same total mass  $\alpha$
- ▶ For multimodal densities in  $\mathcal{C}$ , better to consider the Highest Density Region (HDR): the region with given proportion  $\alpha$  of the total mass and with minimum (Euclidean) volume; equivalently the set:

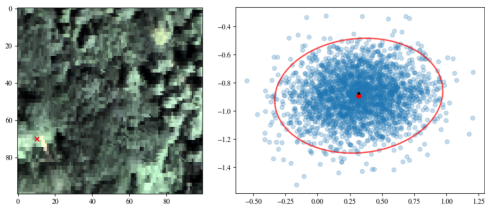
$$H_t = \{\mathbf{x} \in \mathcal{C}, p_{X|Y}(\mathbf{x}|\mathbf{y}) \geq t\}$$

with  $t$  chosen such that

$$\int_{H_t} p_{X|Y}(\mathbf{x}|\mathbf{y}) d\mathbf{x} = \alpha$$

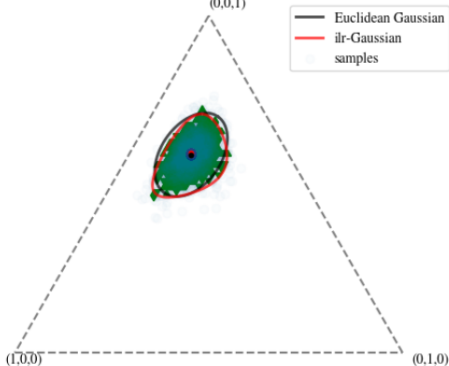
# Pixel-wise Uncertainty

$(1, 0, 0)$ : Broadleaf,  $(0, 1, 0)$ : Conifer,  $(0, 0, 1)$ : Grass



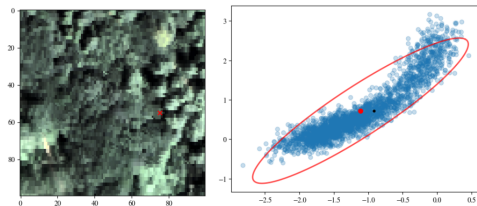
Highest Density 95% Credible Region

$(0,0,1)$

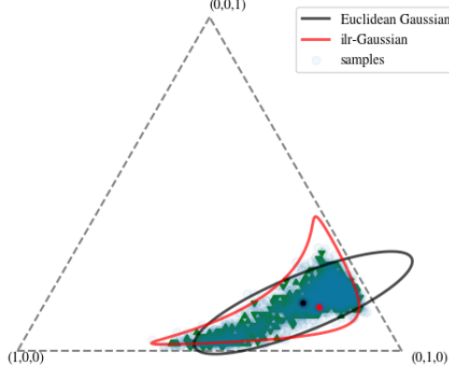


# Pixel-wise Uncertainty

$(1, 0, 0)$ : Broadleaf,  $(0, 1, 0)$ : Conifer,  $(0, 0, 1)$ : Grass

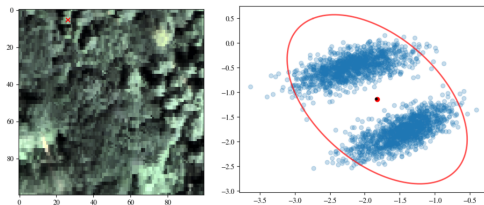


Highest Density 95% Credible Region  
 $(0,0,1)$

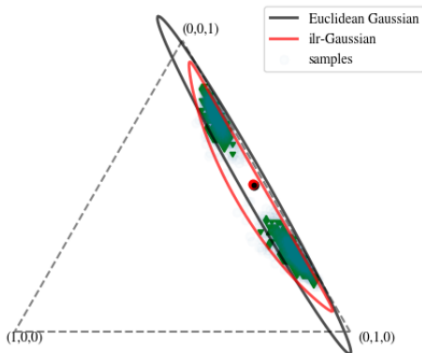


# Pixel-wise Uncertainty

$(1, 0, 0)$ : Broadleaf,  $(0, 1, 0)$ : Conifer,  $(0, 0, 1)$ : Grass

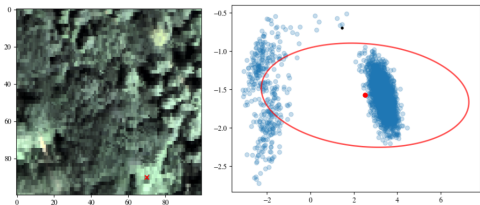


Highest Density 95% Credible Region

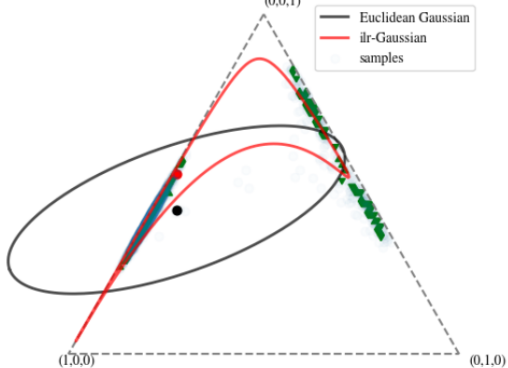


# Pixel-wise Uncertainty

$(1, 0, 0)$ : Broadleaf,  $(0, 1, 0)$ : Conifer,  $(0, 0, 1)$ : Grass



Highest Density 95% Credible Region  
 $(0,0,1)$



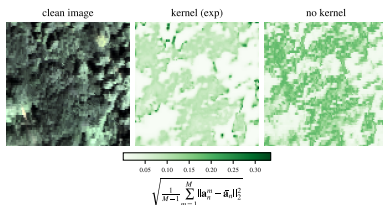
# Spatializing Uncertainty in C

So far we can only do UQ at the pixel level. We need a scalar in each pixel to be able to spatialize the uncertainty.

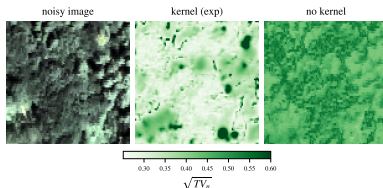
Total variance is one candidate, either in Euclidean or ilr space:

$$\text{Var}_X = \text{tr}(\Sigma_X), \quad \text{Var}_Z = \text{tr}(\Sigma_Z)$$

$\text{Var}_X$  is sensitive to large coordinate-wise changes:



$\text{Var}_Z$  is sensitive to large fold changes (in the log ratios between components):



# Nonlinearity/Multimodality diagnostics

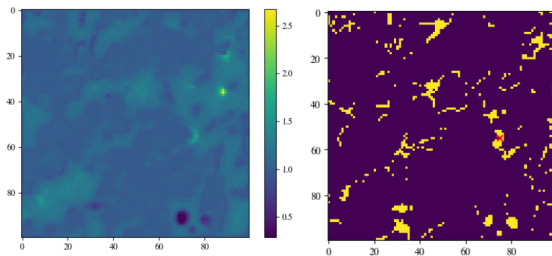
Most pixels have unimodal, similar looking densities in both spaces. This happens when softmax behaves almost linearly (e.g. for concentrated densities not too far from the center)

→ Detect nonlinearity/multimodality by comparing Euclidean total variance and its "prediction" by propagating the ilr-covariance by a linearized  $\text{ilr}^{-1}$  around the mean value:

$$\Sigma_{X_{lin}} = \mathbf{J}_{\mu_Z} \Sigma_Z \mathbf{J}_{\mu_Z}^T$$

where  $\mathbf{J}_{\mu_Z}$  is the Jacobian of  $\text{ilr}^{-1}$  calculated around the posterior ilr-mean.

→ A ratio  $\frac{\text{tr}(\Sigma_X)}{\text{tr}(\Sigma_{X_{lin}})}$  far away from 1 means nonlinearity, possibly multimodality.



Trace ratio (left). Binarized version (large deviations from 1 only), removing pixels too close to the boundary

# Conclusion

- ▶ Natural class of prior distributions on constrained domains diffeomorphic to Euclidean spaces
- ▶ Allows to define constrained Gaussian processes for spatialized priors
- ▶ Also allows for pixel and image level UQ metrics
- ▶ Application to spectral unmixing

# Perspectives

- ▶ Hypothesis testing on variance ratio
- ▶ Define better UQ diagnostics for multimodality, confidence, model misspecification...
- ▶ Construction allows to do more than just GP on  $\mathcal{C}$ : transport the Euclidean vector space structure
- ▶ Integrate into more realistic unmixing pipelines and analyze results with practitioners
- ▶ Same framework also applies to separate epistemic/aleatoric uncertainty in Bayesian Classification (e.g. Bayesian) logistic regression.
- ▶ Extend to other spaces and exploit applications